Indoor Positioning via Three Different RF Technologies

Philipp Vorst, Jürgen Sommer, Christian Hoene, Patrick Schneider, Christian Weiss, Timo Schairer, Wolfgang Rosenstiel, Andreas Zell, Georg Carle

Computer Science Department, University of Tübingen, Tübingen, Germany

Abstract

The continuous tracking of mobile systems via active or passive RFID is a desirable but difficult to achieve objective. In this paper, we present our experimental results of positioning techniques using passive UHF RFID, Bluetooth, and WLAN. We thereby employ three orthogonal measuring techniques: detection rates, signal strength, and round trip time. The orthogonality of the methods is designed to achieve robustness to noise and unforeseen changes in the surroundings. Moreover, due to their different read ranges, the technologies can complement each other at different scales of the environment.

1 Introduction

In many scenarios of everyday life and especially in warehousing and logistics, it is highly desirable to locate objects or persons quickly and accurately. In clinics and factories, for example, staff or mobile systems like transport containers or autonomous vehicles should be located and tracked rapidly. Locating and tracking objects is especially demanding indoors, as the global positioning systems GPS, GLONASS or Galileo fail there.

In this paper we depict three different positioning techniques, which cost-efficiently exploit existing radio infrastructure: passive RFID, Bluetooth, and WLAN. They have in common that the corresponding sensor nodes (RFID tags, Bluetooth nodes, and wireless network adapters) use radio waves for identifying themselves. All three RF standards are used for different purposes, but are usually operated simultaneously indoors.

In addition, our approaches explicitly make use of the different sensor properties: For RFID, we determine tag detection rates; for Bluetooth, we measure the signal strength (RSSI) received from Bluetooth nodes; and for WLAN, we measure the round trip times between WLAN devices in order to estimate distances between them. The orthogonality of the methods and RF technologies is supposed to increase the robustness to noise and unforeseen changes in the environment.

In this publication we assume the following scenario: A mobile system, which can be a carried laptop, a robot, a palette, or anything large enough to have a power supply of its own, has the task to locate itself. RFID, Bluetooth and WLAN landmarks with known IDs and positions are placed in the environment. Then, the system uses the landmarks to locate itself and potentially other nearby objects. Of course, this scenario can be easily extended, e.g. to tracking goods via a given sensor infrastructure.

We conducted experiments with the different positioning methods. Fig. 1 gives an overview of the employed standards, measurement variables, and localization techniques. While we are focusing on the operational range and accuracy of the three methods, future work will combine these three technologies in order to further increase accuracy and robustness.

This paper is organized as follows: First, we elaborate the three positioning techniques via RFID (Sect. 3), Bluetooth (Sect. 4), and WLAN (Sect. 5). We compare the results achieved with the different methods in Sect. 6 and finally draw conclusions in Sect. 7.

2 Background

2.1 Fields of Application

The notion of context-awareness in ubiquitous computing systems and the desire to track goods or localize people has raised the interest in the positioning of mobile systems. By the latter, we subsume humans carrying some kind of communicating devices, mobile objects which should be tracked, and autonomous mobile systems like robots and autonomous vehicles. Today, a broad spectrum of different positioning techniques and technologies for location-awareness has evolved, of which a comprehensive overview is given in [1]. In our publication, we focus on advanced methods which exploit radio frequency (RF) communication between the participating ubiquitous computing devices, since one can expect a coexistence of different types of RF technologies, independent of the target domain and even at the very same spatial location. This applies to a large number of scenarios, for instance supermarkets and warehouses as well as logistics, production, health care, or information services in public areas.

In many of these scenarios, it is desirable to locate systems *accurately*, i.e. their positions should be narrowed down better than only to a coarse area such as a room or an entire building. For example, a person should be guided to a specific object in a densely occupied room. Or, a robot may serve as a shopping guide and inform a customer about nearby objects in a warehouse. The latter application is advanced, but realistic, as other studies show [2, 3].

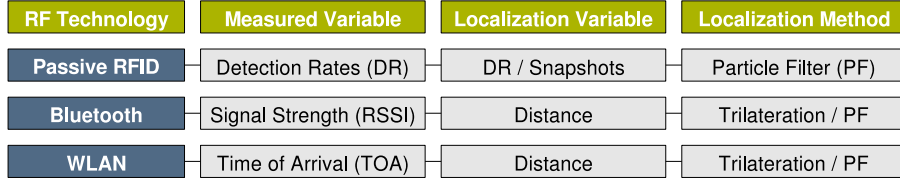Hence, we go beyond cell-based positioning, in which the

RF Technology	Measured Variable	Localization Variable	Localization Method
Passive RFID	Detection Rates (DR)	DR / Snapshots	Particle Filter (PF)
Bluetooth	Signal Strength (RSSI)	Distance	Trilateration / PF
WLAN	Time of Arrival (TOA)	Distance	Trilateration / PF

Figure 1 Overview of our approaches: We apply a specific chain of modeling and localization techniques to each RF technology with its own physical characteristics. The steps are detailed in the corresponding sections of this paper.

location of a mobile system is only determined by the proximity of ambient sensors such as WLAN devices, Bluetooth nodes, or RFID tags. We rather aim at locating and tracking a system in metric coordinates as accurately as possible. Dependent on what RF technology is provided in the area of interest, the mobile system can use RFID, WLAN, and/or Bluetooth for positioning. The three different technologies are supposed to complement each other, since they can be used simultaneously [4], but can be installed in different densities of coverage. Moreover, they have different read ranges (passive UHF RFID of up to 7 m, Bluetooth up to 15 m or more, and WLAN up to 100 m), allowing for localization at different levels of scale. Before we detail our three RF-based localization approaches, we will briefly explain *particle filtering* for the reasons of the self-containedness of this paper. This method enables us to pursue the goal of robust, accurate positioning and to incorporate the employed sensor technologies.

2.2 Particle Filtering

Particle filtering [5] is a widespread Bayesian filtering technique. The state of a system is represented by a finite set of *samples* (also called *particles*) which approximate an arbitrary probability density over the space of potential states of the system. For positioning purposes, the state of the system is the location of a mobile system, and each sample represents a weighted pose hypothesis. Formally, the pose $\mathbf{r}_t$ of the system is represented by a set of n particles, where each particle consists of a pose hypothesis $\mathbf{r}_t^i = (x_t^i, y_t^i)$ and a weighting factor w_t^i. t is a time index referring to the state of the system at time step t. (x_t^i, y_t^i) are the coordinates of the mobile device in a global frame of reference. w_t^i states the importance of the i-th particle. If the direction of motion is provided as in our studies, the current heading θ_t^i of the mobile system can also be added to the state. The actual pose estimate $\mathbf{r}_t$ is computed by $\mathbf{r}_t = \sum_{i=1}^{n} w_t^i \mathbf{r}_t^i$. Motion commands are applied to the particles and change their positions. This is called the *prediction* step. It requires a model of the system's motion, formally given by a probability density $p(\mathbf{r}_t | \mathbf{o}_{t-1}, \mathbf{r}_{t-1})$, where $\mathbf{o}_{t-1}$ is a vector which describes the latest movements. Typically, one will update the particle positions by the motion vector $\mathbf{o}_{t-1}$ (which can be unknown for a human, because it may be hard to predict) and add some random noise which captures the uncertainty about the new position.

By incorporating sensor data $\mathbf{z}_t$, the weights of the samples are corrected according to the likelihood that the associated pose hypothesis explains the current sensor measurements well. This is the *correction* step. Again, formally some likelihood function $p(\mathbf{z}_t | \mathbf{r}_t)$ is used to correct the weights w_t^i via

$$w_t^i = \eta \cdot w_{t-1}^i \cdot p(\mathbf{z}_t | \mathbf{r}_t^i). \qquad (1)$$

Here, η is a normalizing constant, which ensures that $\sum_{i=1}^{n} w_t^i = 1$.

By repeatedly performing prediction and correction over time, the location of a mobile system can be estimated recursively. This evolution is depicted in Fig. 2. Particles close to the true pose receive higher weights in the correction step and therefore contribute more to the pose estimate. Because some pose hypotheses turn out to be unlikely over time, the sample set is *resampled* after the correction step. This means that particles with low weights are removed and replaced by particles near samples with higher weights. Formally, a new set of n particles with equal weights $1/n$ is obtained from the old one by drawing n times a sample from the old set of particles, where the probability of choosing particle i corresponds to its weight w_t^i.

Particle filtering has turned out to be a robust and versatile technique for estimating system states probabilistically. It can be adapted to a large number of applications, e.g. to the positioning problem with different RF technologies as in this paper. Particle filtering performs even well in presence of non-Gaussian noise and highly imprecise measurements. These adverse conditions especially hold for RFID or the WLAN time-of-arrival measurements, for instance.

3 RFID-based Positioning

In our RFID-based positioning approach, a mobile system is equipped with an RFID reader, while stationary RFID tags (transponders) serve as uniquely identifiable landmarks with known positions. This is in contrast to many other proposed methods of RFID usage: There the RFID reader is stationary and tagged goods are moved through a field covered by its antennas. At the entrances of storehouses, for instance, stationary RFID readers would normally detect palettes that are labeled with RFID tags and moved through the antenna gates.

The basic principle of RFID-based positioning is that a mobile system knows its coarse position if it detects a tag whose location is known. Our approach, however, goes beyond this kind of cell-based, qualitative positioning and
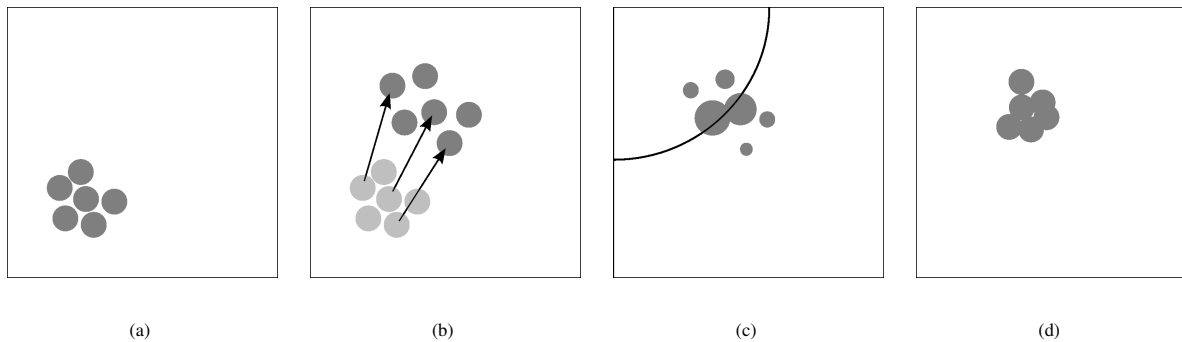
| | | | |
| (a) | (b) | (c) | (d) |

Figure 2 Principle of particle filtering: Each particle is represented by a circle, and its weight is symbolized by the size of the circle. (a) The particles are located near the previous position estimate and have uniform weights. (b) The estimated motion is applied, the particles are shifted correspondingly. Due to the uncertainty in the modeled motion, some noise is added. (c) The particles are weighted according to the likelihood of the arriving sensor data. In this case, we have depicted the sample case of a range measurement (as provided by our Bluetooth and WLAN approaches), denoted by the great black circle. (d) Resampling: Particles with higher weights are replicated, those with lower weights diminish.

aims at a more fine-grained position estimation in metric coordinates, as we will elaborate below.

In this work we use the inexpensive passive UHF (868 MHz) tags of the standard EPC Class 1 Generation 2. Our research is motivated by the expectation that in the near future many quasi-stationary objects in warehouses, supermarkets, and logistics will be marked with RFID tags.

What makes passive UHF technology less attractive, however, is the problem that the detection of a tag highly depends on its orientation and on nearby objects which absorb or reflect the transmitted electromagnetic waves. Thus, even tags within the read range (of up to 7 m) are often not detected. Even worse, if a transponder has successfully been detected, one only knows that it is close and hence the mobile system must be within a radius of 7 m around the detected transponder. In opposition to sensors such as laser range finders, neither distance nor bearing to the tag are provided by the RFID reader.

The solutions of other research groups are to use short range RFID and place transponders in the floor [6], to use active RFID with signal strength information [7, 8, 9] (see also Sec. 4), or to fuse RFID with vision [8]. Our solution to these challenges, however, is two-fold: First, we exploit the abovementioned fact that tag detection rates – averaged over a series of measurements – are conditioned by the relative position (distance, angle, height, orientation) of the tag to the antenna of the RFID reader. By this, they give a hint where a detected tag is most likely and – because the positions of some tags are known – also the mobile system. Fig. 3 visualizes the dependency of tag detection rates on the relative position from the robot.

Second, we apply particle filtering as described in Sect. 2.1. This allows to refine and track the pose of a mobile system over time, although RFID data arrive quite rarely (at less than 2 Hz) and are subject to noise. For our studies, we utilized the mobile robot which is depicted in Fig. 6. The use
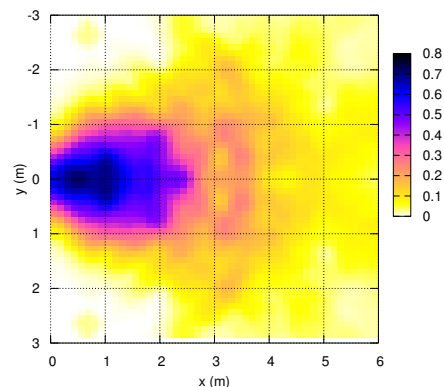

Figure 3 Learned RFID sensor model: Tag detection rates are conditioned on the relative position of a tag to an RFID antenna. The antenna is located in the origin and scans tags on the right hand side.

of particle filtering with RFID sensor data and the exploitation of RFID detection rates was first proposed by Hähnel et al. [10]. What is new in our approach is that we employ two different observation models, developed in our group, in order to assign likelihoods to particles: Either we use a semi-automatically learned model or we apply a fingerprinting technique called RFID snapshots.

For the first model, we learn tag detection rates with an autonomous mobile robot [11]. The robot traverses the environment, records RFID measurements for tags with known positions, and finally estimates the tag detection probabilities. In this training phase, the reference positions of the robot are determined by an accurate laser-based localization system. A resulting model is shown in Fig. 3. It estimates the probability $q(\mathbf{r}_{rel})$ of detecting a tag whose relative position from the RFID antenna is denoted by $\mathbf{r}_{rel}$. Although in this case the model is confined to the 2-D relative

coordinates of RFID tags and our robot, it can be extended to other relevant parameters, e.g. the relative height and orientation. Note that while in this work the gained model is used for positioning purposes, it could also be utilized to optimize the placement of RFID readers in plants and supermarkets as well as to check specified antenna characteristics and transponder performance.

The crucial step for localization is how to reweight the particles (cf. Sect. 2.1). Here, we assume that for each RFID antenna, the reader supplies a list $\mathbf{z}_t = (l_1, l_2, \ldots)$ of tags which have been detected. Given the learned model, the solution is straightforward: For any particle i and known position of a tag l, we compute the relative position $\mathbf{r}_{t,rel}^{i,l}$ between the tag and the RFID antenna mounted on the robot. Then, the sensor model directly states the likelihood of detecting the tag: $p(\mathbf{z}_t|\mathbf{r}_t^i) = q(\mathbf{r}_{t,rel}^{i,l})$. Localization results turned out to be more accurate if likelihoods are only computed for tags l that have been detected in the current measurement and the non-detections of known tags are ignored.

The second approach by Schneegans [12] is based on fingerprinting: Short series of RFID measurements, so-called RFID snapshots, are taken at reference positions in the environment during a training phase. Series means that not only one inquiry is initiated but rather N inquiries. Thus, the result is not a list $\mathbf{z}_t = (l_1, l_2, \ldots)$ of singly detected tags but a list of $\mathbf{z}_t = (f_{l_1}, f_{l_2}, \ldots)$ counting how often the tag l_j has been detected. This list of detected tags represents the signature (fingerprint) of the reference position, at which it was recorded and is assumed to characterize that specific position well.

When the mobile system is to be localized later, its position is determined by comparing the current snapshot with the recorded fingerprints. Technically, this comparison is embedded in the evaluation of a likelihood function again: The detection probability $\hat{q}_l(\mathbf{r}_t^i)$ for each tag l can be estimated by a linear combination of recorded training snapshots, conditioned on the position $\mathbf{r}_t^i$ of the i-th particle. Now taking N inquiries into account, the likelihood can be computed from the binomial distribution

$$p(\mathbf{z}_t|\mathbf{r}_t^i) = \prod_{l \in \mathbf{z_t}} \binom{N}{f_l} \hat{q}(\mathbf{r}_{t,rel}^{i,l})^{f_l} (1 - \hat{q}(\mathbf{r}_{t,rel}^{i,l}))^{N-f_l}.$$

A similar fingerprinting approach based on passive RFID was presented by Lim and Zhang [13], but their solution was non-probabilistic, and they attached transponders to the ceiling at regular distances.

Both approaches, the semi-automatically learned model and the fingerprinting technique, use RFID detection rates for pose estimation and are embedded in particle filters, but note the difference between them: The model-based approach requires an explicit sensor model and the positions of some reference tags to be known. The snapshot-based approach, on the other hand, does not require an explicit sensor model and need not know the positions of RFID tags. However, it has to learn fingerprints and their respected positions before the actual localization phase.
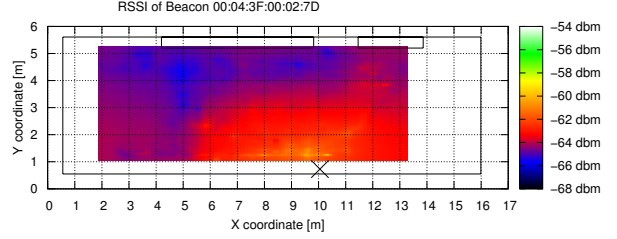

Figure 4 Received signal strength (in dBm) between a sender (black cross) and a receiver (colored area).

Computationally, both methods have similar requirements with respect to positioning on-line. For details, we refer the reader to [12].

4 Bluetooth Signal Strength-based Positioning

Various mobile devices and sensor nodes such as the BT-node by ETH Zürich are equipped with Bluetooth radio transceivers. Because of the read range of about 15 m, they are not precise enough to consider just the reachability of the sensor nodes as in the RFID-based approach. Thus, for positioning, it is suggested to employ received signal strength indications (RSSI) [14, 15, 16, 17], because the RSSI value decreases with distance between sender and receiver. Fig. 4 demonstrates the relative signal strength between two Bluetooth sensor nodes placed in our laboratory. As the distance between sender (black cross) and receiver increases, also the received signal strength decays. The RSSI values allow for a fine-grained resolution and therefore high accuracy. For region and cell based approaches the reader is referred to [18, 19, 20] and [21, 22, 23], respectively.

Measuring the RSSI, we still need to estimate the distance. To calculate the distances d_j between sender and receiver, we apply an attenuation model which takes the sending power P_{tx} of the mobile node, the signal measurements from the anchor nodes P_{rcv_j} and the path loss coefficient α into account:

$$d_j = \sqrt[\alpha]{C \frac{P_{tx}}{P_{rcv_j}}} \qquad (2)$$

Path loss α and the constant C must be calibrated prior to the positioning experiments.

To locate the position of an object, multiple landmarks are required: In our experiments we used seven landmarks and conducted RSSI measurements in Bluetooth connection mode. With the increasing proliferation of RF communication technologies coexistence issues have to be taken into consideration. Since the ISM band is license-free, other wireless standards make use of the spectrum furthermore. In order to coordinate the measurements and transmissions of our Bluetooth anchor nodes piconet time-slot scheduling was applied. Therefore a round robin polling mechanism is applied, where the node to be located is in
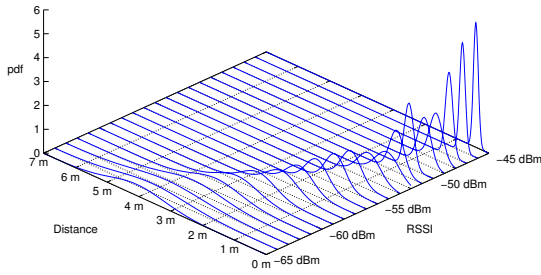
Figure 5 Probability density functions of distances for different signal strength values within the interval -45 dB to -65 dB.

Figure 6 Measuring the distance between source and destination via the DATA/ACK packet sequence.

master role, sending its downlink packet to each beacon slave. The beacon is polled to send an up-link packet with current RSSI measurements. For m beacons each beacon is polled every $1250/m$ μs.

The ranging process, where RSSI values are mapped to distance estimations described above is based upon imprecise sensor data, which are sensitive to noise and other isotropic effects like shadowing or attenuation behind objects or multipath fading. Fig. 5 shows the typical characteristics of several probability density functions (pdf) of distances for signal strength-based range estimation. For this illustration the numbers of occurences of distances were counted for given RSSI values from -45 dB to -65 dB. In this interval the standard deviation is increasing from 15 cm to 1.5 m. We observed in preliminary experiments that it is reasonable to estimate the standard deviation $\sigma(d)$ by $\hat{\sigma}(d) = 0.4 \cdot d$.

In the *correction step* of the particle filter new weights are calculated using a Gaussian likelihood function. Thereby, the distance estimates from the landmarks are integrated. For range-based positioning, the observations $\mathbf{z}_t$ are the distance estimates $\mathbf{d}_t = (d_{1,t}, d_{2,t}, \ldots, d_{m,t})$ at time t. After calculating the distance $d_{j,t}$ for each beacon j located at $\mathbf{b}_j$, using the path attenuation model described by Eq. 2, the new weights are determined by

$$p(\mathbf{z}_t|\mathbf{r}_t^i) = \prod_{j=1}^{m} \frac{1}{\hat{\sigma}(d_{j,t}) \cdot \sqrt{2\pi}} \cdot e^{-\frac{1}{2}\left(\frac{||\mathbf{b}_j - \mathbf{r}_t^i|| - d_{j,t}}{\hat{\sigma}(d_{j,t})}\right)^2}. \quad (3)$$

This likelihood function is used in Eq. 1; the importance of each particle is weighted according to how well the distance of that particle from the positions of the Bluetooth landmarks is explained by the RSSI-based distance estimates. Using RSSI and the particle filter, our solution provides a robust indoor positioning system for medium range distances.

5 Wi-Fi TOA-based Positioning

Currently, various commercial active RFID tags use IEEE 802.11 [24] technologies. For example, Aeroscout adopted standard Wi-Fi wireless networks to accurately locate and
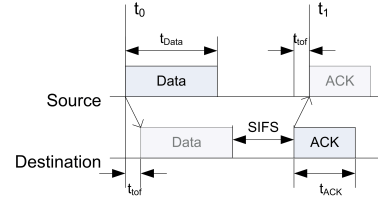
manage assets and people [25]. Their product line and the BTnodes described above use RSSI to determine the position of WLAN nodes [26]. To enhance RSSI, we follow an alternative approach based on the time of arrival (TOA) of transmission signals. Location tracking based on time of arrival algorithms measures the duration of the propagation of the physical transmission signal, which travels at the speed of light through free space. As compared to RSSI measurements, TOA has the benefit that its measurement results scale linearly with the open-air propagation distances.

If the physical transmission signal is echoed by the tags, a two-way TOA approach is possible that does not require precise clocks. In previous work it has been proposed to use the IEEE 802.11 data transmission for two-way TOA to estimate the distances between WLAN nodes [27, 28]. Two-way TOA takes advantages of a feature of the IEEE 802.11 protocol. By default, the receiver answers an error-free decoded IEEE 802.11 DATA packet immediately with an ACK packet. These DATA and ACK packet sequences can be applied to range measurements (Fig. 6). The time of flight (TOF) is then calculated as

$$t_{tof} = \frac{1}{2}\left(t_1 - t_0 - t_{DATA} - t_{SIFS}\right).$$

Knowing the speed of light, the distance between two nodes can be calculated. However, a single TOF measurement is usually not precise enough. Instead, it is required to average the measurement results of multiple observations. Having the distance, trilateration can be used to determine the relative positions of objects. Unlike triangulation, which uses angle measurements to calculate the subject's location, trilateration uses the known locations of two or more landmarks, and the measured distance between the subject and each reference point.

As an extension to enhance the positioning performance, we invented a four-way TOA measurement algorithm [29], which utilizes a common feature of IEEE 802.11. Frequently, IEEE 802.11 does not only send two packets (such as data and ACK) but multiple packets in a sequence. For example, if the RTS/CTS mode is switched on, every data packet is preceded by a RTS and CTS packet. Similar, if the data packet is slitted, the data fragments are transmitted in a row. Even the upcoming IEEE 802.11n standards require to send multiple packets in sequence in order to conduct an adaptation to the link layer quality and to tune their
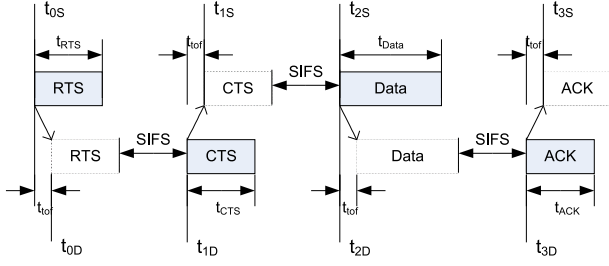
Figure 7 Measuring the distance between source and destination via four-way TOA using the RTS/CTS/DATA/ACK packet sequence.

MIMO antennas. Using the RTS/CTS/Data/ACK packet sequence depicted in Fig. 7, we can calculate the transmission duration using the following two formulas and then average the results of all round trip time (RTT) observations.

$$t_{tof} = \frac{1}{2}\left(t_{1S} - t_{0S} - t_{RTS} - t_{SIFS}\right)$$

$$t_{tof} = \frac{1}{2}\left(t_{3S} - t_{2S} - t_{DATA} - t_{SIFS}\right)$$

Using these round trip time estimates and applying them to the trilateration, we can easily calculate the position as described in [29].

We have implemented these algorithms in the open-source software "Goodtry" [30]. Goodtry is a pure software solution using common WLAN hardware and does not require modified WLAN chip sets. However, mature Wi-Fi trilateration will take advantage of slightly enhanced chip sets, which ease the implementation of round trip time measurements. We are aware of at least one chip set currently in development that will support round trip time measurements with a high temporal precision. Until this chip set becomes available, we have to stick to off-the-shelf hardware.

Under these circumstances testing the Wi-Fi trilateration algorithm is difficult because every aspect of the experimental setup must be strictly controlled. In order to judge the precision of our solution, an elaborate laboratory setup was required.

We placed six anchors (landmarks) in our laboratory, as depicted in Fig. 8. The anchors are actually based on LinkSys WRT54GL access points, which we reprogrammed with the Linux operating system OpenWRT. During the experiments, access points were operating in ad-hoc mode using a constant transmission rate (11 MBps) and a long PLCP preamble. If all access points (APs) are operated in ad-hoc mode, we can communicate more easily to them without the need to switch the channels. Thus, we prefer the ad-hoc against the "normal" basic service set (BSS). A constant transmission rate and using only the long preamble causes the packets to have a constant transmission duration. If the packets do not have a constant transmission duration, the clock drift of the communication nodes fal-
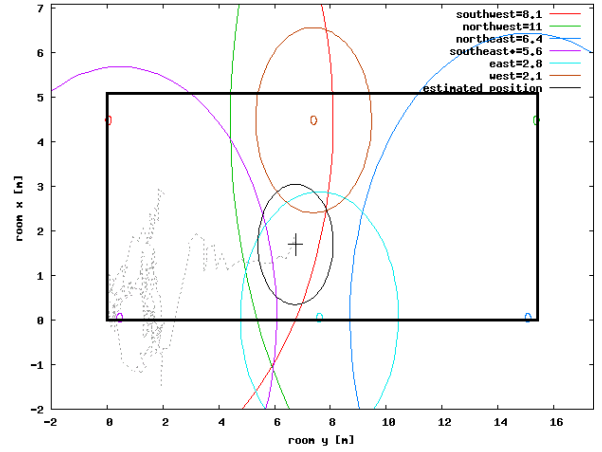

Figure 8 An example of WLAN trilateration. The black rectangle represents the dimensions of our laboratory. The small circles refer to the six access points. The larger colored circles around the APs show the distance estimates between APs and the robot. The black cross is the estimated position of the robot. This position estimate has an estimated error displayed by the black circle.

sify the results causing a measurement error that is far too high to be useful.

On the robot, we installed two WLAN cards. The first one transmits ICMP pings to the six APs. Pings are control packets, which are immediately echoed by the receivers at the IP network protocol layer. The other one listens to the transmissions. We use an Atheros Communications PCI card as transmitting WLAN. As a monitor, we use an old Atheros card with the chip set AR5212. Only a few WLAN cards can act as monitor because the TOA algorithms require precise time stamps. The selected chip set (beside Prism2 and Prism 54 chip sets) is the only currently available WLAN solution which provides us with a time resolution of 1 μs.

Electromagnetic waves (such as light or WLAN packets) travel within one microsecond about 300 meters in open-air. For indoor Wi-fi trilateration a measurement resolution of 300 meters is far too high. Using four-way TOA, we can reduce the resolution to 75 meters because the packets have traveled four times the distances. A further improvement is achieved if multiple round trip time measurements are combined and averaged. Then, an interesting effect can be noticed that has been described in [28, 31]. Because the clocks of the WLAN card are slightly drifting, the measurement results oscillate over time and do not remain constant. If using multiple results, the negative effect of time quantization can be eliminated entirely. For example, if we take the mean of 500 to 2000 pings, we achieve a precision that is far better than 300 meters.

The WLAN cards have to be selected in a way that their clocks are slightly drifting. During the setup of the experiments we found out that even WLAN card of different

Figure 9 Experimental platform: An RWI B21 mobile robot with an UHF RFID reader by Alien Technology, two pairs of RFID antennas (white), and a laser range finder (blue, mounted in front of the robot) for reference localization. The WLAN and Bluetooth antennas are mounted on top of the robot.

vendors work at very similar (<10 ppb) frequencies. The results presented in this paper are based on a WLAN card that has a clock frequency offset of 15 ppm as compared to the APs.

Overall, one can say that conducting TOA measurement with current off-the-shelf hardware is quite cumbersome and fragile. However, we expect that future chip sets will provide much better support making WLAN trilateration a promising technology.

With regard to the particle filter, we use a similar likelihood function as for Bluetooth (see Eq. 3). Let $\mathbf{w}_j$ denote the positions of the m WLAN access points serving as landmarks and $d_{j,t}$ be the estimated distance to AP j at time t, then

$$p(\mathbf{z}_t|\mathbf{r}_t^i) = \prod_{j=1}^{m} \frac{1}{\sigma \cdot \sqrt{2\pi}} \cdot e^{-\frac{1}{2}\left(\frac{||\mathbf{w}_j - \mathbf{r}_t^i|| - d_{j,t}}{\sigma}\right)^2}. \quad (4)$$

The constant σ was determined in preliminary experiments, in which we observed a standard deviation of the estimation errors of approx. 3 m.

6 Results

We conducted a series of experiments in order to measure the positioning accuracies of our approaches. The experiments were performed with a robot as a mobile platform, for which there were two reasons: Firstly, accurate reference positions are provided by an onboard laser-based localization system. By this, we can thoroughly measure the positioning errors of the presented methods. And secondly, the experiments were embedded in a scenario in which we use the robot for automatic inventory purposes [32].

Besides the reference positioning system, the robot is equipped with three hardware devices required for our RF-based positioning methods: an off-the-shelf UHF RFID reader (868 MHz), a WLAN IEEE 802.11g interface, and two

Bluetooth interfaces. The latter two are mounted on top of the robot. The RFID antennas span an angle of approx. $90°$, which lets them scan for RFID tags both to the front and the sides.

All experiments were conducted in a laboratory. The laboratory has a size of approx. $90\,\mathrm{m}^2$, of which the robot can visit $50\,\mathrm{m}^2$ of free space. We attached 24 passive UHF RFID tags to desks and walls at distances of 1-2 m. Seven Bluetooth nodes were installed at an average distance of approx. 3 m in similar places near the tags. Moreover, we mounted six WLAN access points close to the ceiling, four in the corners of the room and two in the middle. The precise locations of the RFID tags, Bluetooth nodes, and WLAN access points were measured manually. Additionally to the 24 stationary RFID tags of known positions, we placed a supermarket shelf with approx. 400 RFID-tagged product packages in the center of the laboratory. The positions of these tags were not mapped, but could be memorized by the RFID snapshots technique.

As experimental data, we recorded 15 sets of sample trips through the laboratory, in which both the laser-based reference positions and the sensor data from RFID, Bluetooth (11 sets containing both types of data), and WLAN (the remaining 4 sets) were saved.

For these studies, we considered particle filter-based *tracking* only, i.e. an approximate guess of the initial pose of the robot was given. This is justified by our experience that the non-particle filter-based trilateration methods (e.g. MMSE, see [14]) can provide suitable coarse initialization. Moreover, by increasing the number of particles, the initialization can also be implemented right in the particle filter, which we tested in earlier studies. In these experiments, however, we wanted to focus on the tracking capabilities of our methods.

The particle filter was comprised of 300 samples for the model-based methods (RFID detection rates, Bluetooth RSSI and WLAN TOA). The motion model was the same for all methods. Only for the WLAN-based positioning approach, we added zero-mean Gaussian noise with a standard deviation of 0.1 m between any two measurements. The reason for this was that due to the noisy nature of TOA distance measurements, hardly any particle would reflect the estimated distance; the tracked trajectory would mainly represent the estimated motion (odometry) of the robot.

On each trajectory, the particle filter was run ten times for each of the three RF technology-based approaches. Note that particle filtering is a probabilistic method and has an inherent random nature, which requires to run the algorithms several times in order to achieve statistical significance. Moreover, we also incorporated the motion estimates of the robot in the motion model of the particle filter. This typically increases the accuracy compared to modeling the hardly predictable motion of a human being.

The results listed in Tab. 1 show that RFID and Bluetooth allow for tracking at a mean absolute positioning error of approx. half a meter, sometimes better. The direct comparison between the two methods is interesting because they

Method	Mean ± Std.dev.	Median	90th percentile
RFID	0.432 ± 0.095	0.435	0.527
Bluetooth	0.494 ± 0.149	0.474	0.678
WLAN	3.315 ± 0.738	3.545	4.274

Table 1 Mean absolute positioning errors (in meters) for the three technologies. For RFID, the model-based approach was pursued here.

yield comparable accuracies. This is even though signal strength information is provided for Bluetooth, whereas there is distance supplied for a single RFID measurement. On the other hand, there were more RFID landmarks (24 tags vs. 7 Bluetooth nodes). But this ratio was supposed to reflect that passive RFID tags can be expected to appear at a much higher density in RF infrastructures.

The accuracy of our WLAN approach is lower. But recall that the precision of WLAN hardware clocks in principal is able to measure multiples of 300 meters only. That is why the listed tracking results can be regarded surprisingly accurate. Note that further experiments will follow and the investigated scenario covers a small area of free space only. We also performed experiments with RFID snapshots. They yielded a mean absolute positioning error of 0.264 m ± 0.047 m (median 0.267 m). The caveat here, however, is that due to fingerprinting, the snapshots also contained valuable information about dozens of tags in the shelf which were not used in the model-based approach. That is why one must not directly compare the results obtained by the two RFID-based methods. To compensate for the extra information memorized in the fingerprints, we had the snapshot technique not only tracked, but also localized globally, i.e. localized without initial pose estimate. As a consequence, we had to increase the number of particles for this method to 2000. Based on the given results for the snapshots, one can draw the conclusion that quite accurate positioning (even including global positioning) is possible with passive RFID by means of fingerprinting. Yet, one must argue that taking RFID snapshots requires a quite accurate reference positioning system.

7 Conclusion

In this paper, we have presented three different RF-based techniques which can be used to determine the positions of persons or mobile objects. They base on the evaluation of tag detection rates of passive UHF RFID tags, RSSI measurements of Bluetooth nodes, and TOA measurements of WLAN devices. We presented the results obtained from tracking a mobile robot with sensor data from those three RF technologies and odometry data (motion estimates). For RFID and Bluetooth, we obtained tracking accuracies of half a meter or better, while WLAN TOA measurements yielded an accuracy of a few meters. All single techniques reveal their individual strengths with respect to positioning accuracy and read range: While RFID and Bluetooth seem suitable for rather accurate position-

ing over short distances, WLAN can be used for positioning over longer distances at a coarser level of granularity. A combination of all three technologies promises even improved positioning performance for future work. Forthcoming experiments will also include larger scenarios and different densities of the sensor nodes.

Since low-cost and off-the-shelf hardware is used, our approaches are cost-efficient and exploit existing RFID, Bluetooth, and WLAN infrastructures. The accuracies are (still) inferior to high performance ultra-wide-band or laser-based positioning methods, but the depicted methods represent a good compromise between cost and accuracy.

8 Acknowledgments

9 References

[1] K. Muthukrishnan, M. Lijding, and P. Havinga. *Location- and Context-Awareness*, volume 3479/2005 of *Lecture Notes in Computer Science*, chapter Towards Smart Surroundings: Enabling Techniques and Technologies for Localization, pages 350–362. Springer Berlin/Heidelberg, May 2005.

[2] A. Bley, H.-M. Groß, and M. Söffge. Assistenzrobotik wird alltagstauglich - Shoppingroboter kommt im Baumarkt an. Press release by MetraLabs GmbH, Technische Universität Ilmenau, and toom Baumarkt GmbH, June 2007. (in German).

[3] V. Kulyukin, C. Gharpure, and J. Nicholson. RoboCart: Toward Robot-Assisted Navigation of Grocery Stores by the Visually Impaired. In *Proceedings of the 2005 IEEE/RSJ International Conference on Intelligent Robots and Systems (IROS 2005)*, Edmonton, Alberta, Canada, 2005.

[4] Q. Pang and V.C.M. Leung. Channel clustering and probabilistic channel visiting techniques for wlan interference mitigation in bluetooth devices. *IEEE Transactions on Electromagnetic Compatibility*, 49(4):914–923, Nov. 2007.

[5] A. Doucet, S. Godsill, and C. Andrieu. On sequential Monte Carlo sampling methods for Bayesian filtering. *Statistics and Computing*, 10:197–208, 2000.

[6] J. Bohn. Prototypical implementation of location-aware services based on super-distributed RFID tags. In *Proceedings of the 19th International Conference on Architecture of Computing Systems (ARCS 2006)*, number 3894 in LNCS, pages 69–83. Springer-Verlag, 2006.

[7] K. Yamano, K. Tanaka, M. Hirayama, E. Kondo, Y. Kimuro, and M. Matsumoto. Self-localization of Mobile Robots with RFID System by using Support Vector Machine. In *Proceedings of the IEEE/RSJ International Conference on Intelligent Robots and*

Systems (IROS 2004), volume 4, pages 3756–3761, Sept/Oct 2004.

[8] H. Chae and K. Han. Combination of RFID and Vision for Mobile Robot Localization. In *Proceedings of the 2005 International Conference on Intelligent Sensors, Sensor Networks and Information Processing*, pages 75–80, 2005.

[9] J. Djugash, S. Singh, and P.I. Corke. Further Results with Localization and Mapping using Range from Radio. In *Proceedings of the International Conference on Field & Service Robotics (FSR '05)*, July 2005.

[10] D. Hähnel, W. Burgard, D. Fox, K. Fishkin, and M. Philipose. Mapping and Localization with RFID Technology. In *Proceedings of the 2004 IEEE International Conference on Robotics and Automation (ICRA 2004)*, pages 1015–1020, 2004.

[11] P. Vorst and A. Zell. *European Robotics Symposium 2008*, volume 44/2008 of *Springer Tracts in Advanced Robotics*, chapter Semi-Autonomous Learning of an RFID Sensor Model for Mobile Robot Self-localization, pages 273–282. Springer Berlin / Heidelberg, February 2008.

[12] S. Schneegans, P. Vorst, and A. Zell. Using RFID snapshots for mobile robot self-localization. In *Proceedings of the 3rd European Conference on Mobile Robots (ECMR 2007)*, pages 241–246, Freiburg, Germany, September 19-21 2007.

[13] A. Lim and K. Zhang. *Advances in Applied Artificial Intelligence*, volume 4031 of *Lecture Notes in Computer Science*, chapter A Robust RFID-Based Method for Precise Indoor Positioning, pages 1189–1199. Springer Berlin / Heidelberg, 2006.

[14] S. Subramanian, J. Sommer, S. Schmitt, and W. Rosenstiel. SBIL: Scalable indoor localization and navigation service. In *WCSN '07: Third International Conference on Wireless Communication and Sensor Networks*, pages 27–30, 2007.

[15] C. di Flora, M. Ficco, S. Russo, and V. Vecchio. Indoor and outdoor location based services for portable wireless devices. In *ICDCSW '05: Proceedings of the First International Workshop on Services and Infrastructure for the Ubiquitous and Mobile Internet (SIUMI)*, pages 244–250, Washington, DC, USA, 2005. IEEE Computer Society.

[16] A. Madhavapeddy and A. Tse. A study of bluetooth propagation using accurate indoor location mapping. In *Ubicomp*, pages 105–122, 2005.

[17] K. Wendlandt, P. Robertson, and M. Berbig. Indoor localization with probability density functions based on bluetooth. In IEEE, editor, *PIMRC 2005*, pages 2040–2044. VDE Verlag, 09 2005.

[18] J.O. Filho, A. Bunoza, J. Sommer, and W. Rosenstiel. Self-localization in a low cost bluetooth environment. In *Proceedings of the 5th International Conference on Ubiquitous Intelligence and Computing (UIC 2008)*, LNCS 5061. Springer-Verlag Berlin/Heidelberg, June 2008.

[19] A. Galstyan, B. Krishnamachari, K. Lerman, and S. Pattem. Distributed online localization in sensor networks using a moving target. In *Proceedings of the Third International Symposium on Information Processing in Sensor Networks (IPSN '04)*, pages 61–70, New York, NY, USA, 2004. ACM Press.

[20] S. Guha, R. Murty, and E.G. Sirer. Sextant: a unified node and event localization framework using non-convex constraints. In *Proceedings of the 6th ACM International Symposium on Mobile Ad Hoc Networking and Computing (MobiHoc '05)*, pages 205–216, New York, NY, USA, 2005. ACM Press.

[21] M. Nilsson, J. Hallberg, and K. Synnes. Positioning with Bluetooth. In *10th International Conference on Telecommunications ICT 2003*, pages 954–958, 2003.

[22] F. Forno, G. Malnati, and G. Portelli. Design and implementation of a bluetooth ad hoc network for indoor positioning. *IEE Proceedings - Software*, 152(5):223–228, 2005.

[23] G. Anastasi, R. Bandelloni, M. Conti, F. Delmastro, E. Gregori, and G. Mainetto. Experimenting an indoor bluetooth-based positioning service. In *ICDCSW '03: Proceedings of the 23rd International Conference on Distributed Computing Systems*, page 480, Washington, DC, USA, 2003. IEEE Computer Society.

[24] Wireless LAN medium access control (mac) and physical layer (phy) specifications. *IEEE Std 802.11-2007*, 2007.

[25] Aeroscout web page. http://www.aeroscout.com, April 2008.

[26] P. Bahl and V. Padmanabhan. RADAR: An in-building RF-based user location and tracking system. In *INFOCOM 2000*, Tel-Aviv, Israel, 2000.

[27] D. D. McCrady, L. Doyle, H. Forstrom, T. Dempsey, and M. Martorana. Mobile ranging using low-accuracy clocks. *Microwave Theory and Techniques, IEEE Transactions on*, 48(6):951, 2000. 0018-9480.

[28] A. Günther and C. Hoene. Measuring round trip times to determine the distance between wlan nodes. In *Networking 2005*, Waterloo, Canada, 2005.

[29] C. Hoene and J. Willmann. Four-way toa and software-based trilateration of IEEE 802.11 devices. submitted, January 2008.

[30] C. Hoene. Goodtry - Software based WLAN Trilateration. http://sourceforge.net/projects/goodtry, June 2008. To be published.

[31] K.I. Ahmed and G. Heidari-Bateni. Improving two-way ranging precision with phase-offset measurements. *Global Telecommunications Conference (GLOBECOM '06). IEEE*, pages 1–6, Nov. 2006.

[32] T. Schairer, C. Weiss, P. Vorst, J. Sommer, C. Hoene, W. Rosenstiel, W. Straßer, A. Zell, G. Carle, P. Schneider, and A. Weisbecker. Integrated scenario

for machine-aided inventory using ambient sensors. In *Proceedings of the 4th European Workshop on RFID Systems and Technologies (RFID SysTech 2008)*, Freiburg, Germany, June 10-11 2008.

Philipp Vorst studied computer sciences at RWTH Aachen University in Aachen, Germany, and received his master's degree (Diplom) in 2006. Since then, he has been a Ph.D. candidate with University of Tübingen, Germany, at the Department of Computer Architecture led by Prof. Andreas Zell. His research focuses on mobile robotics and navigation methods using RFID technology. Contact: philipp.vorst@uni-tuebingen.de

Jürgen Sommer studied electrical engineering, philosophy and computer science, and received his master's degree (M.A.) at the University of Tübingen, Germany, in 2006. Since then, he has been a Ph.D. candidate with University of Tübingen at the Department of Computer Engineering led by Prof. Wolfgang Rosenstiel. He works on the design and evaluation of sensor networks. Contact: jsommer@informatik.uni-tuebingen.de

Christian Hoene studied in the TKN Group at Technical University of Berlin. In 2005, he finished his Ph.D. studies on voice over WLAN. Currently, he is a postdoc at the Computer Networks and Internet group led by Prof. Georg Carle at the University of Tübingen, Germany. His research covers Internet-based voice communication, wireless transmissions, location tracking, accounting, and charging. He is in charge of the technical and organisatorial mangement of the AmbiSense project. Contact: hoene@uni-tuebingen.de